A R C H I V E S O F M E T A L L U R G Y A N D M A T E R I A L S
Volume 56 2011 Issue 2
DOI: 10.2478/v10172-011-0035-7

W. WOŁCZYŃSKI*, T. OKANE**, C. SENDEROWSKI***, B. KANIA****, D. ZASADA***, J. JANCZAK-RUSCH*****

META-STABLE CONDITIONS OF DIFFUSION BRAZING

METASTABILNE WARUNKI SPAJANIA DYFUZYJNEGO

A thermodynamic justification for the joint formation is developed on the basis of the diffusion brazing of the Ni/Al/Ni system. The phenomena of dissolution and solidification were included into the description. The first solid/solid transformation is also discussed. Mainly, a description for the isothermal brazing occurrence in the meta-stable conditions is developed. It involves the application of the criterion of higher temperature of the solid / liquid (s/l) interface. The dissolution of the filler metal in the substrate is described by the N_0 – solute concentration within the dissolution zone (liquid film) distinguished at the substrate surface. The selection of the N_0- parameter by the dissolution is justified by the *Thermocalc* calculation of the Ni-Al phase diagram for meta-stable equilibrium. According to the model assumptions, the solidification is accompanied by partitioning or by undercooled peritectic reaction resulting in formation of the intermetallic phase. The average Al – solute concentration measured across some $Al_3Ni_2/Al_3Ni/Al_3Ni_2$ joints confirms that the N_0 - solute concentration is conserved within the analyzed joint sub-layers. The Ni-Al phase diagram for meta-stable equilibrium referred to the solidification is also calculated by means of the *Thermocalc Software*. It allows locating the solidification path, s/l interface path and redistribution path onto the mentioned diagram. Superposition of both calculated phase diagrams is also given to show that the joint formation occurs cyclically under the meta-stable conditions.

Keywords: meta-stable equilibrium, joint formation model, dissolution, solidification

Zaproponowano termodynamiczne uzasadnienie dla kształtowania się złącza na przykładzie spajania dyfuzyjnego systemu Ni/Al/Ni. Do proponowanego opisu włączono zjawiska rozpuszczania i krystalizacji. Pierwsza przemiana w stanie stałym również poddana jest dyskusji. Głównie, opis dotyczy przebiegu spajania dyfuzyjnego w warunkach metastabilnych. Wymaga on zastosowania kryterium wyższej temperatury frontu krystalizacji. Rozpuszczanie składnika łączącego (Al) w podłożu (Ni) jest opisane stężeniem N_0 w strefie rozpuszczania (w ciekłej błonce wyróżnionej tuż przy powierzchni podłoża). Selekcja parametru N_0 jest uzasadniona obliczeniami z użyciem program *Thermocalc Software* Programem tym wyznaczono diagram fazowy Ni-Al dla równowagi metastabilnej odniesiony do zjawiska rozpuszczania. Zgodnie z założeniami proponowanego opisu krystalizacji towarzyszą rozdział składnika lub przechłodzona reakcja perytektyczna skutkujące formowaniem się fazy międzymetalicznej. Średnie stężenie Al zmierzone w złączach $Al_3Ni_2/Al_3Ni/Al_3Ni_2$ potwierdza, że stężenie N_0 jest zachowane w podwarstwach analizowanych złącz. Również, wyznaczono diagram fazowy Ni-Al dla równowagi metastabilnej odniesiony do krystalizacji. Wykorzystano ponownie program *Thermocalc Software.* Pozwoliło to na zlokalizowanie ścieżki krystalizacji, ścieżki frontów krystalizacji, ścieżki redystrybucji na diagramie fazowym równowagi metastabilnej. Superpozycja obydwu obliczonych diagramów jest także pokazana celem zilustrowania, iż formowanie się złącza zachodzi cyklicznie w obserwowanych warunkach metastabilnych.

Nomenclature

dx	infinitesimal amount of the substrate melted due to the dissolution of the liquid Al solute, [mole fr.],
i	index of the range of solidification; $i = 1$ for the range $N_0 \Rightarrow N_1$; $i = 2$ for the range $N_1 \Rightarrow N_2$; $i = 3$ for the range $N_2 \Rightarrow N^F$, (phase diagram for stable equilibrium), Figure 3,
k_i	partition ratio varying with the concentration of solute in the liquid, $i = 1, \ldots, n$, [mole fr./mole fr.],

* INSTITUTE OF METALLURGY AND MATERIALS SCIENCE, POLISH ACADEMY OF SCIENCES, 30-059 KRAKÓW, 25 REYMONTA STR., POLAND
** AIST – NATIONAL INSTITUTE OF ADVANCED INDUSTRIAL SCIENCE & TECHNOLOGY, UMEZONO 1-1-1, 305 8568 TSUKUBA, JAPAN
*** MILITARY UNIVERSITY OF TECHNOLOGY, KALISKIEGO 2, 00-908 WARSZAWA, POLAND
**** AGH – UNIVERSITY OF SCIENCE & TECHNOLOGY, FACULTY OF PHYSICS AND ADVANCED INFORMATICS, 30-059 KRAKÓW, 19 REYMONTA STR., POLAND
***** EMPA – SWISS FEDERAL LABORATORIES FOR MATERIALS SCIENCE & TECHNOLOGY, UEBERLAND 129, 86 000 DUEBENDORF, SWITZERLAND

k_i^0 first component of the partition ratio independent of any changes in the solute concentration along *liquidus* line, $i = 1, \ldots, n$, [mole fr./mole fr.],

k_i^L second component of the partition ratio independent of any changes in the solute concentration along the *liquidus* line, $i = 1, \ldots, n$, [mole fr./mole fr.],

L^0 amount of the liquid at the start of solidification, usually $L^0 = 1$, [dimensionless],

l_i^0 amount of the liquid at the beginning of a given range of solidification, i, $i = 1, \ldots, n$, Eq. (1A), [mole fr.],

N_i^B solute redistribution after both partitioning and back-diffusion, $i = 1, \ldots, n$, Eq. (5P), Eq. (5C), [mole fr.],

N^F concentration of the filler metal in its liquid solution at the T^T temperature, [mole fr.],

N_i^L solute concentration in the liquid, observed along the *liquidus* line for a given range of solidification, (local solidification path), $i = 1, \ldots, n$, Eq. (1), Eq. (1P-3P), Eq. (1C-3C), [mole fr.],

N_i^S solute concentration at the solid / liquid interface, observed along the *solidus* line for a given range of solidification, (local solid/liquid interface path), $i = 1, \ldots, n$, Eq. (4P), Eq. (4C), [mole fr.],

N_0 solute content at the beginning of solidification path (on *liquidus* line), [mole fr.],

$\hat{N}_0$ average solute concentration measured across the formed multi-layer, [mole fr.],

N_1 solute concentration in the liquid at the first peritectic reaction (phase diagram for stable equilibrium), Figure 3, [mole fr.],

N_2 solute concentration in the liquid at the second peritectic reaction (phase diagram for stable equilibrium), Figure 3, [mole fr.],

N_2^M solute concentration in the liquid at the peritectic reaction (phase diagram for the meta-stable equilibrium), Figure 9, [mole fr.],

N_i solute concentration in the liquid at a given peritectic reaction (phase diagram for stable equilibrium), Figure 3, Eq. (2), $i = 1, 2$, [mole fr.],

$N_{(i-1)}$ solute concentration in the liquid at a given peritectic reaction, (for $i = 2, 3$) or solute concentration at the beginning of solidification path (for $i = 1$), (phase diagram for stable equilibrium), Eq. (1), Figure 3, [mole fr.],

N^s solute concentration within the zone s, (Figure 9), [mole fr.],

N^{ss} solute concentration within the zone ss, (Figure 9), [mole fr.],

N_{min} solute concentration at the minimum of *liquidus* line, phase diagram for meta-stable equilibrium, Figure 8, Figure 9, [mole fr.],

n number of ranges of solidification for a given solidification path, $n = 3$,

s zone of saturation created in the substrate,

ss zone of super-saturation created in the substrate,

T_f^* temperature at the solid / liquid interface of a given phase / compound, f, $f \equiv AlNi, Al_3Ni_2, Al_3Ni$ (in short, $f \equiv 11, 32, 31$)) as it results from the intersection of a given meta-stable *solidus* line with the line which denotes N_0 concentration, [K],

T_{11}^* temperature of the AlNi phase solid /liquid interface, Figure 7, [K],

T_{32}^* temperature of the Al_3Ni_2 phase solid /liquid interface, Figure 7, [K],

T_D temperature at which the minimum of *liquidus* line appears in the phase diagram for meta-stable equilibrium, Figure 8, [K],

T_R real temperature of bonding (temperature of the interconnection formation), [K],

T^T melting temperature of the Al – filler metal, [K],

t^K time of the solidification progress, Figure 5a, [s],

t^F time at which solidification is completed, Figure 5b, Figure 13, [s],

t time, [s],

t_M time of the beginning of the first solid / solid transformation, Figure 13, [s],

$t_3 1^B$ time of the birth of the Al_3Ni phase within the Ni/Al/Ni interconnection, Figure 13, [s],

X^0	amount of the solid at a given stage (progress) of solidification when the process is arrested and morphology frozen, (calculated for a total system along a global solidification path) [dimensionless],
x	current amount of the solid, [dimensionless],
x_i	amount of the primary phase which takes part in a given peritectic reaction at the $i-th$ range of solidification, $i = 1, \ldots, n$, [dimensionless],
x_i^0	amount of the solid at a given stage (progress) of solidification when the process is arrested and morphology frozen, (calculated for a given $i-th$ range of solidification along a local solidification path), [dimensionless],
x_i^{max}	sum of amounts of both primary phase remaining after peritectic reaction and peritectic phase resulting from the peritectic reaction at a given solidification range, $i = 1, \ldots, n$, [dimensionless],
x_i^{min}	amount of the primary phase remaining after the peritectic reaction at a given range of solidification $i = 1, \ldots, n$, [dimensionless];
$x_i^{max} - x_i^{min}$	denotes the amount of peritectic reaction product obtained at a given range of solidification, $i = 1, \ldots, n$,, [dimensionless]; a given peritectic reaction occurring at the N_i solute concentration (as observed on *liquidus* line) is treated as belonging to the $i-th$ range of solidification, (stable equilibrium phase diagram),
α_i^D	back-diffusion parameter for both partitioning and redistribution, $i = 1, \ldots, n$, [dimensionless],
β_i^{ex}	redistribution extent coefficient, $i = 1, \ldots, n$, defined in details by Wołczyński *et al.* [3], [dimensionless],
β_i^{in}	redistribution intensity coefficient, $i = 1, \ldots, n$, defined in details by Wołczyński *et al.* [3], [dimensionless],
λ_1^F	thickness of the Al_3Ni_2 phase sub-layer within the interconnection formed at time t^F, Figure 5, [μm],
λ_2^F	half the thickness of the Al_3Ni phase sub-layer within the interconnection formed at time t^F, Figure 5, [μm],
λ_1^K	thickness of the Al_3Ni_2 phase sub-layer within the interconnection formed at time t^K, Figure 5, [μm],
λ_2^K	half the thickness of the Al_3Ni phase sub-layer within the interconnection formed at time t^K, Figure 5, [μm].

1. Introduction

A solidification, a dissolution and some solid/solid transformations are predicted by Tuah-Poku, *et al.*, [1] as phenomena to be observed during diffusion brazing. The solidification and dissolution are subjected to consideration in the current model. However, exceptionally the first solid / solid transformation is strictly connected with solidification and dissolution, through the mass balance, Kloch *et al.*, [2].

A dissolution of substrate by the liquid filler metal occurs continuously within a zone dx Figure 1. The dissolution prepares the liquid film within the zone dx. Once the zone becomes liquid the mass of this liquid film diffuses towards the joint symmetry axis and solidification occurs at the s/l interfaces, Wołczyński *et al.*, [3].

Solidification is accompanied by the undercooled peritectic reactions, Figure 2. According to the concept of Chuang *et al.*, [4], undercooled peritectic reactions take place at the solid/liquid (s/l) interface.

The occurring of peritectic reactions at the s/l interface of cells, formed within a given sub-layer, are marked schematically with some arrows in Figure 2. Mainly, the internal channels within cells are employed for the flow of dissolved substrate towards the s/l interfaces (bulk diffusion). The dissolved substrate contained within zone dx, has the solute concentration equal to N_0, Figure 1.

Under described conditions, a bonding process can result in a joint that reproduces micro-structurally a sequence of inter-metallic compounds or phases as it is visible in an adequate phase diagram for stable equilibrium, Jacobson and Humpston [5], Jiangwei *et al.,* [6] and Wołczyński *et al.,* [7].

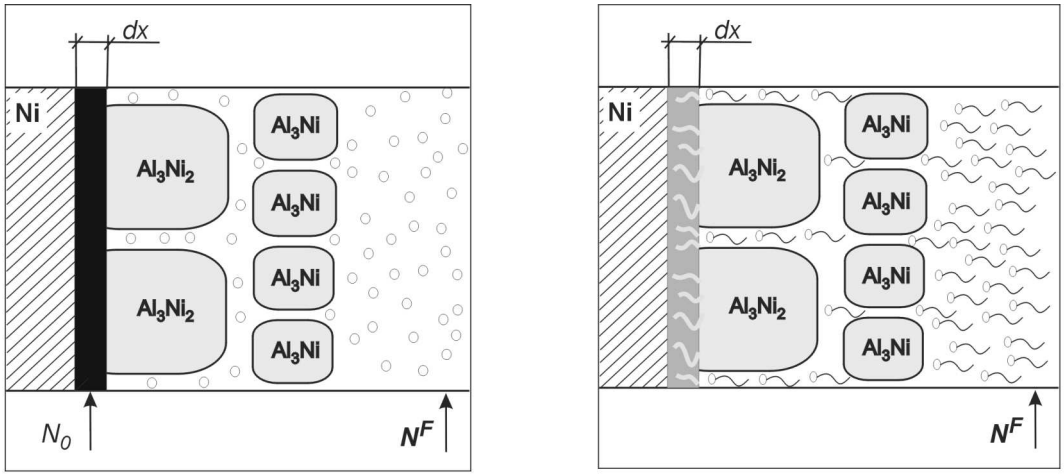

Fig. 1. Ni-substrate dissolution within its infinitesimally small amount, dx (the so-called zone dx situated just at the substrate surface) due to diffusion of liquid solution of the filler metal, N^F, through the channels situated among some cells of Al_3Ni_2 or Al_3Ni phases formed in a given sub-layer, respectively; a/ zone dx is just formed, b/ beginning of the zone dx formation; a reaction within the zone dx is: $liquid(N^F) + Ni \rightarrow undercooledliquid(N_0)$

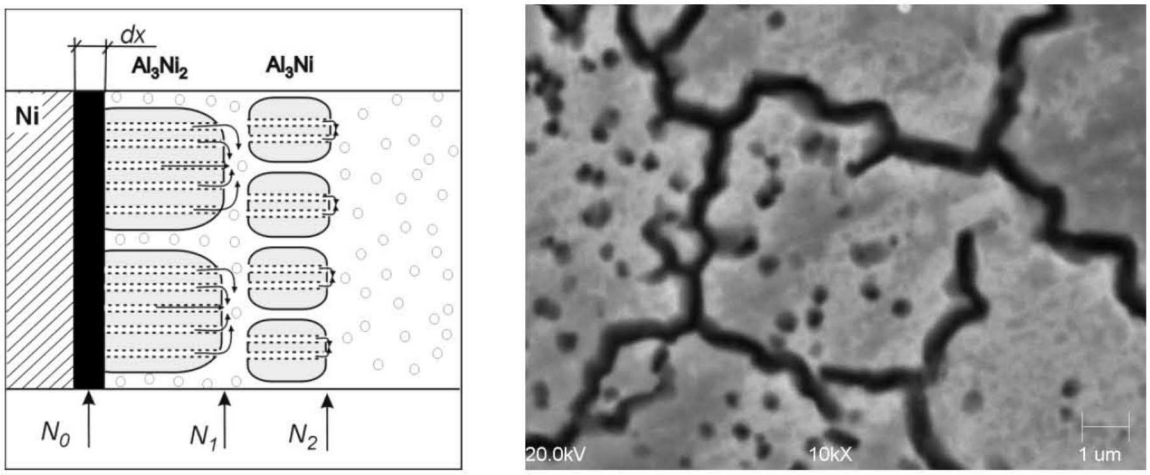

Fig. 2. The undercooled peritectic reactions at the front of cells (as it results from the phase diagram for stable equilibrium): N_1 – solute concentration within undercooled liquid for the first peritectic reaction resulting in formation of the sub-layer that contains cells of the Al_3Ni_2 intermetallic phase, N_2 – solute concentration within undercooled liquid for the second peritectic reaction resulting in formation of the sub-layer that contains cells of the Al_3Ni intermetallic compound; a/ the channels predicted in the model for bulk diffusion are shown schematically and completed with some arrows that signify occurrence of a given peritectic reaction; b/ channels observed at the cross-section of the sub-layer of the δ – phase within the Fe/Zn/Fe system, [8]

The analysis is focused on the formation of the Ni/Al/Ni joints in relation to the diffusion brazing. It makes it possible to develop a description for the solidification preceded by the dissolution and a new explanation for the role of the solidification path for the creation of the joint sub-layers.

Additionally, a thermodynamic justification for the beginning of solidification path, N_0 and the end of solidification path, N^F, both are given. The *Thermocalc Software* calculation of the Ni-Al phase diagram for meta-stable equilibrium will give the grounds for this justification.

2. Description of the $NiAl_3Ni_2/Al_3Ni/Al_3Ni_2$-Ni joint formation

The system selects one and only one nominal concentration of the solute, N_0 at a given temperature, T_R, Kloch *et al.,* [2]. The selection of the N_0 – parameter by the system occurs in such a way to ensure the film, dx, (zone dx), to be liquid. The zone dx is created at the surface of a substrate, Figure 1. It is evident that the liquid layer, dx, is strongly undercooled from its *liquidus* temperature. Thus, dissolution occurs at a given temperature, T_R, as long as it is necessary to transform solid substrate

zone, dx, into the liquid film, dx. Once the dx zone becomes liquid and its concentration achieves selected N_0, the undercooled liquid film is ready to be subjected to solidification involving undercooled meta-stable peritectic reactions, Figure 2.

The average Al-solute content measured within the Ni/Al/Ni joint obtained after different periods of time is always equal to the N_0 – concentration. Thus, the N_0 – parameter is situated on the *liquidus* line as the beginning of solidification path, Figure 3.

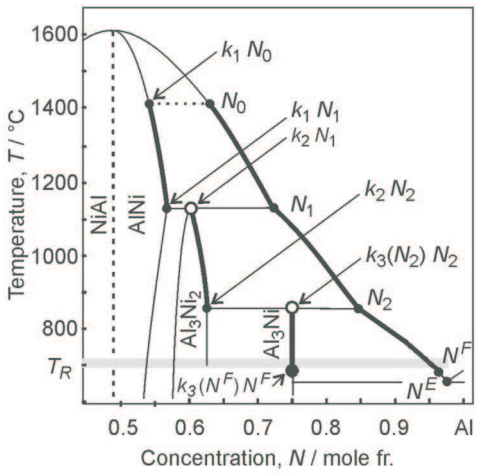

Fig. 3. Ni-Al phase diagram for stable equilibrium with the $N_0 \rightarrow N_1 \rightarrow N_2 \rightarrow N^F$ solidification path and with the $k_1N_0 \rightarrow k_1N_1 \rightarrow k_2N_1 \rightarrow k_2N_2 \rightarrow k_3(N_2)N_2 \rightarrow k_3(N^F)N^F$ "historical", solid / liquid interface path. T_R = 700°C, and N_0 = 0.64 [mole fr.]

According to the current model assumption, the constant partitioning is justified for the formation of an intermetallic phase. In the case of an inter-metallic compound formation a varying partition ratio is to be applied. Thus, the universal definition of the k – partition ratio was introduced:

$$k_i(x) = k_i^0 + k_i^L N_{i-1}/N_i^L(x) \quad i = 1, \ldots, n \tag{1}$$

As the assumed peritectic reaction x_i+liquid(N_i) $\rightarrow \left[x_i^{max} - x_i^{min}\right]$ occurs during solidification, therefore, the amount of the primary phase is to be defined accordingly.

$$\begin{aligned} &x_i(\alpha_i^D, l_i^0, N_{i-1}, N_i, k_i) = \\ &= l_i^0 \left[\left(1 - \left(N_i/N_{i-1}\right)^{(1-\alpha_i^D k_i)/(k_{i-1})}\right)/(1-\alpha_i^D k_i)\right] \end{aligned} \tag{2}$$

Eq. (1) is universal one and can be applied to the descriptions of peritectic reaction when: a/ an intermetallic phase is formed, then $k_i^L = 0$, b/ an intermetallic compound is formed, then $k_i^0 = 0$.

The x_i^{max} and x_i^{min} – parameters are defined in detail by Wołczyński *et al.* [3]. Finally, the model allows determining of the ratio of sub-layers thickness: $\lambda_1^K/\lambda_2^K = x_1^{max}/x_2^{max} + x_3$, Figure 4, with some explanations shown in Figure 5.

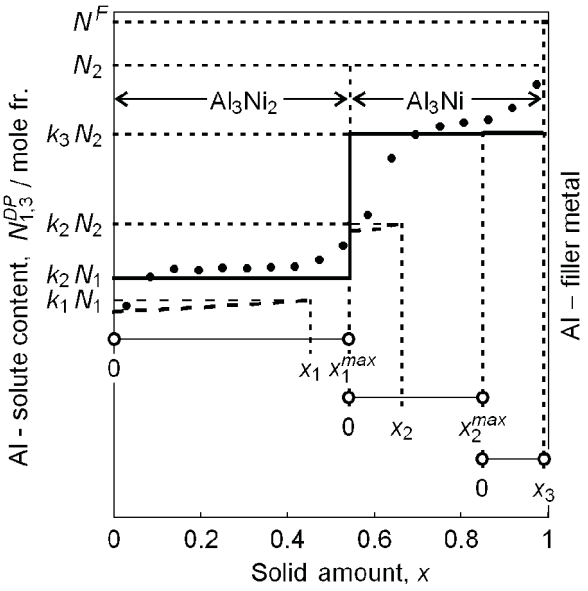

Fig. 4. Reproduction of the sub-layers thickness ratio together with the measured solute redistribution profile resulting from the undercooled peritectic reactions. Theoretical profiles are reproduced across the half a joint Ni / Al_3Ni_2/ Al_3Ni / Al_3Ni_2 / Ni; the ratio of sub-layers is reproduced for the solidification path $N_0 \rightarrow N_1 \rightarrow N_2 \rightarrow N^F$ shown in Figure 3; the measurement points are taken from the EDAX analysis; the solidification was carried out at 700 ^{0}C for 121 s

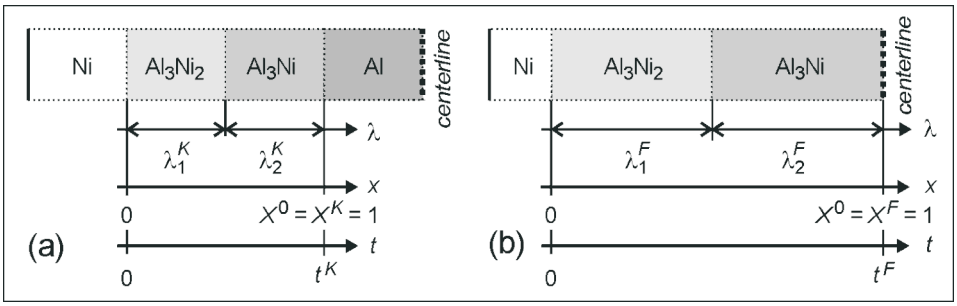

Fig. 5. The meaning of some parameters in solidification of the Al_3Ni_2/Al_3Ni multilayer on the Ni-substrate shown at: a/ a given step of the Al_3Ni_2/Al_3Ni multi-layer formation, b/ completion of the Al_3Ni_2/Al_3Ni multilayer formation

The simulation shown in Figure 4 is obtained as if the formation of joint occurs according to the phase diagram for the stable equilibrium, Figure 3. Some equations applied to the simulation are shown in details in the Appendix, Eqs. (1P-5P) and Eqs. (1G-5G). Additionally, Eq. (2) was used to calculate x_1, x_2 and x_3 parameters. According to the applied phase diagram for stable equilibrium two peritectic reactions were calculated during simulation: $x_1 + liquid(N_1) \rightarrow \left[x_1^{max} - x_1^{min}\right]$ and $x_2 + liquid(N_2) \rightarrow \left[x_2^{max} - x_2^{min}\right]$.

The result of simulation shown in Figure 4 should be the same as the result of simulation based on the phase diagram for meta-stable equilibrium. However, the phase diagram for meta-stable equilibrium should be much more realistic to describe perfectly the phenomena which occur during the formation of joint.

According to the current model, the solute concentration within a given sub-layer is the same as the solute concentration at the peritectic point in the phase diagram. Thus, the Al solute concentration equals 60 at.%, for the Al_3Ni_2 – intermetallic phase and 75 at.% for the Al_3Ni – intermetallic compound.

However, it is to be verified whether the ratio of sub-layers thickness depends on the real temperature, T_R, at which the experiment was performed.

3. Experiment

A set of experiments was carried out in order to study a sequence of the intermetallic sub-layers formation. The experiment of the Ni/Al/Ni diffusion joint formation was performed at different temperatures: 700, 750, 800, 850, 900, 950 and 1000^0C.

An Al-foil 25 μm thick was located between two pieces of nickel then tightened. The Ni/Al/Ni system was put into a vacuum furnace, then heated until a given temperature.

At each of the imposed temperature the Al-foil was melted and the system subjected to dissolution / solidification. The solidification was halted after a given period of time and morphology of the interconnections was frozen, Figure 6.

The Al-solute segregation profiles were analyzed across the frozen interconnections by means of the EDAX – micro-analyzer.

Next, an average content of the Al-solute, $\hat{N}_0$, was determined for each of the studied joint. The estimated results are gathered in Table 1.

TABLE 1
Estimated values of the Al – solute content, $\hat{N}_0$ within the Ni/Al/Ni joints formed at different temperature T_R, due to solidification arrested at time, t, with $t < t^F$.

T_R [^{0}C]	$\hat{N}_0$ [at. %]
700	63.5
750	63.6
800	65.7
850	66.5
900	64.5
950	63.7
1000	62.5

Since the values of the $\hat{N}_0$ – parameter (Table 1) are similar to each other, the average Al – solute content, denoted as $\bar{N}_0$, and representative for all investigated joints was calculated. It is equal to $\bar{N}_0 \approx 0.64$ [mole fr.], $\left(\bar{N}_0 \cong (1/7) \sum \hat{N}_0\right)$.

The revealed interconnections morphology proved that the ratio of sub-layers thickness does not change with the T_R – temperature imposed in a given experiment.

It should be emphasized that according to the mass balance the average solute content, $\bar{N}_0$ revealed in the frozen interconnections should be equal to the initial solute content, N_0, from which the interconnections were formed.

The experiments allowed the identification of the intermetallic compound / phase sub-layers, Figure 6. The areas which contains the N^F – solution are visible in Figure 6a.

The pure Al - areas resulting from the so-called "*mantis phenomenon*" revealed by Wołczyński *et al.* [7], (full consumption of the Al_3Ni compound by the Al_3Ni_2 – dominant phase) and described by the adequate reaction: $2Al_3Ni \rightarrow Al_3Ni_2 + 3Al$, are also visible, Figure 6b.

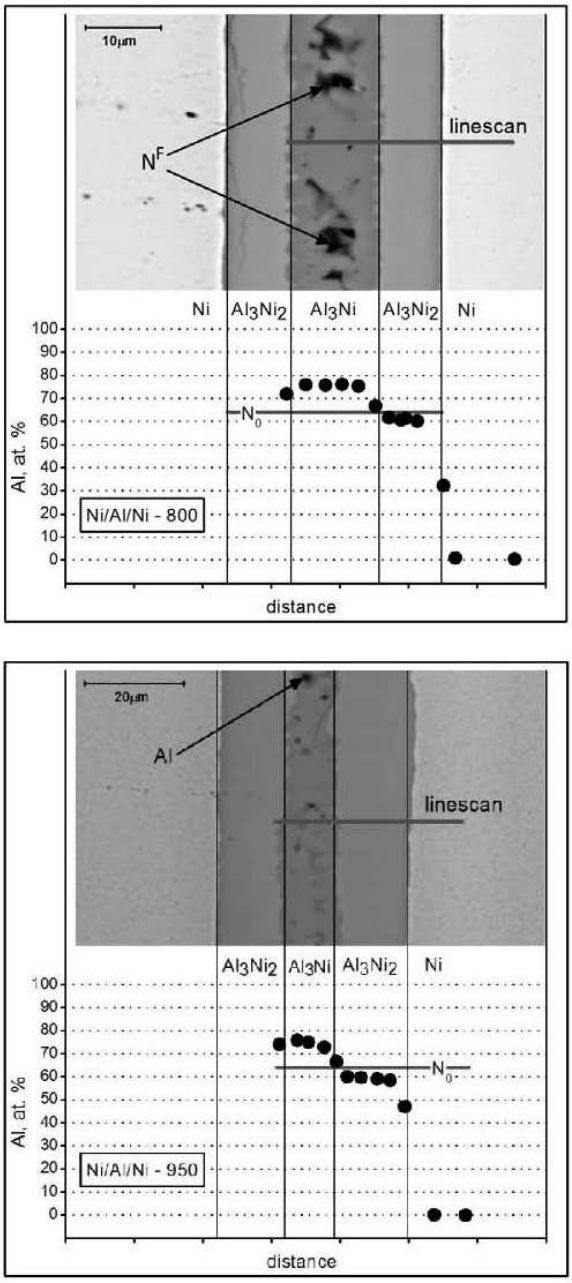

Fig. 6. a.) The Ni / Al_3Ni_2/ Al_3Ni / Al_3Ni_2 / Ni Ni/Al/Ni joint morphology, (T_R = 800°C), as observed at time $t < t^F$; the $\hat{N}_0$ – parameter estimated; b.) The Ni / Al_3Ni_2/ Al_3Ni / Al_3Ni_2 / Ni Ni/Al/Ni joint morphology, (T_R = 950°C), as observed at time $t > t_M$; the $\hat{N}_0$ – parameter estimated

4. Meta-stable condition of the joining technology

N_0 – parameter localization on the *liquidus* line, as shown in Figure 3, indicates that the AlNi phase should be formed as the first sub-layer just at the substrate surface. Meanwhile, experimental observations confirm that the Al_3Ni_2 phase sub-layer is formed, and AlNi phase does not appear during experiment, Figure 6.

It is evident that the solidification occurred under meta-stable conditions since the AlNi phase was not formed.

The transition of the system from stable conditions into meta-stable conditions can be justified by means of the Umeda-Okane-Kurz criterion, (UOK criterion), Umeda *et al.* [9].

The schematically drawn Ni-Al phase diagram for stable equilibrium is shown in Figure 7.

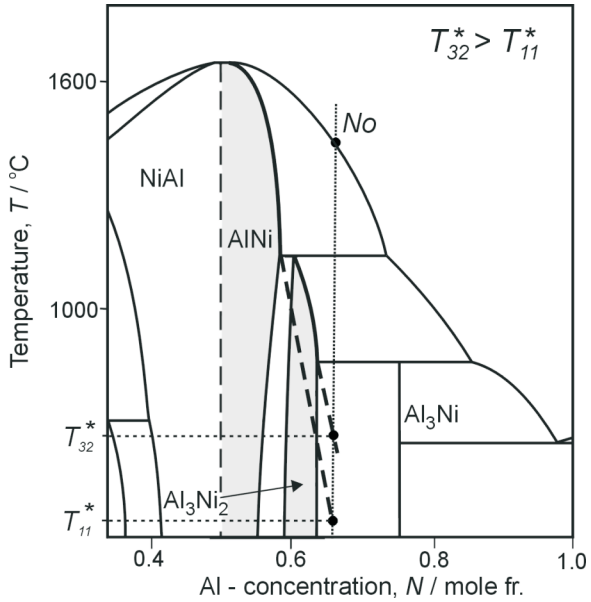

Fig. 7. Application of the UOK criterion to the Ni-Al phase diagram for stable equilibrium; two meta-stable solidus lines are added: first – for AlNi phase and second – for Al_3Ni_2 phase to explain a competition between the phases appearance

The characteristic $\bar{N}_0 = N_0$ – solute content is also situated in the phase diagram. The intersections of the N_0 – content with both meta-stable *solidus* lines defines T_j^* – temperatures of the s/l interface for both discussed phases ($j = AlNi, Al_3Ni_2$).

According to the mentioned criterion this phase is formed which manifests a higher temperature of its s/l interface during solidification. In the case of the Ni-Al system $T_{32}^* > T_{11}^*$ as visible and written in Figure 7. Therefore, the Al_3Ni_2 phase sub-layer is selected by the system instead of expected AlNi phase sub-layer formation.

Additionally, some calculations made by means of the *Thermocalc Software* allowed some Ni-Al phase diagrams for meta-stable equilibrium to be reproduced, respectively: a/ for a dissolution, Figure 8a, b/ for a solidification resulting in formation of both observed phases, Figure 8b.

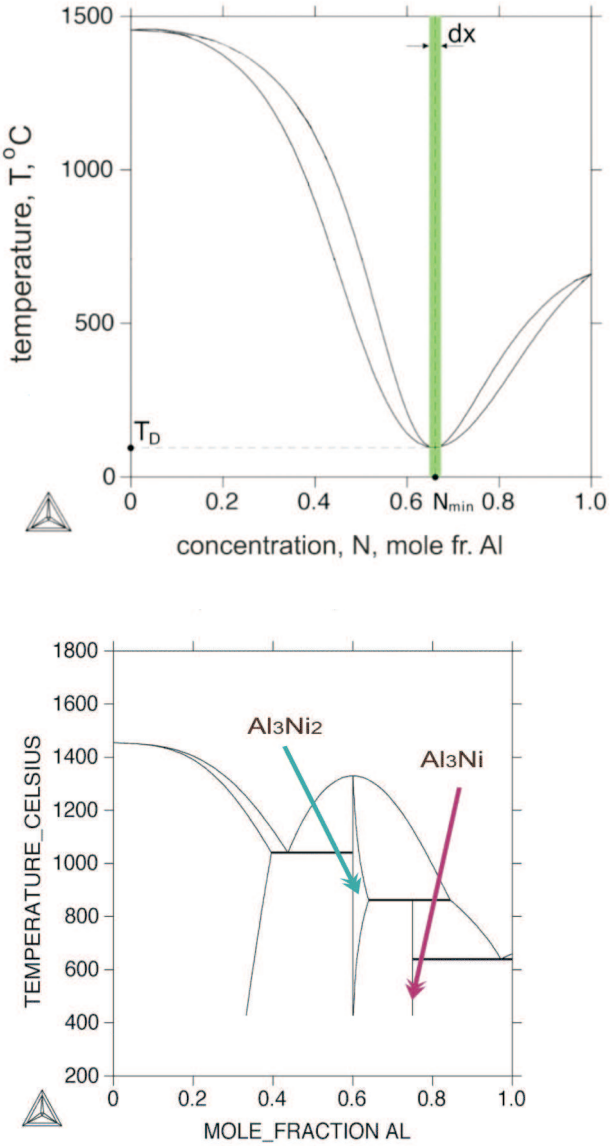

Fig. 8. Ni-Al phase diagram for meta-stable equilibrium calculated for: a/ the solubility of Al (filler metal applied in the technology) in the Ni substrate, b/ for solidification under meta-stable condition

The calculated phase diagram (meta-stable equilibrium) for the dissolution, Figure 8, manifests the minimum at the Al-solute concentration $N_min \approx 0.64$ [mole fr.].

It is evident that the N_min parameter value has the same meaning as the N_0 parameter value that represents dissolution phenomenon in the model described by the scheme shown in Figure 1.

The minimum shown in Figure 8, defines the minimal temperature, T_D. At the T_D – temperature the dissolution (described in Figure 1) occurs as easily as possible. In other words, the appearance of minimum suggests that even at the T_D temperature the liquid solution can exist within the zone dx, Figure 1, under imposed meta-stable condition of the Ni/Al/Ni interconnection formation.

The phase diagram for dissolution is superposed onto the phase diagram for solidification in order to emphasize that both discussed phenomena occur cyclically, dissolution: $N^F \rightarrow N_0$, and solidification: $N_0 \rightarrow N^F$, Figure 9.

The dissolution path, $N^F \rightarrow N_0$ begins at the *liquidus* line of the meta-stable equilibrium phase diagram calculated for solidification and is completed at the *liquidus* line minimum of the meta-stable equilibrium phase diagram calculated for dissolution (dashed green line), Figure 9.

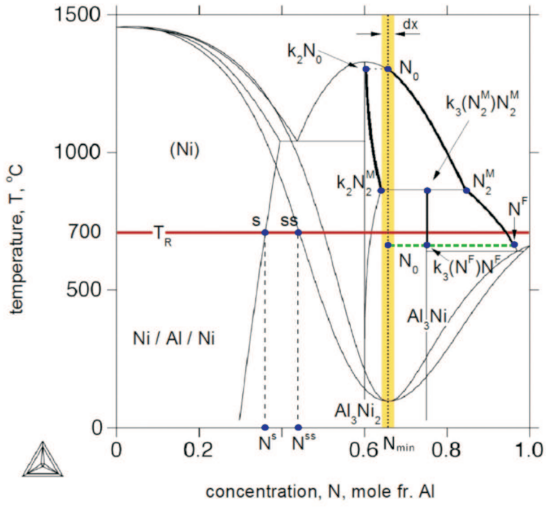

Fig. 9. Superposition of the Ni - Al phase diagrams for meta-stable equilibrium calculated: a/ for the dissolution phenomenon discussed in Figure 8a, and b/ for solidification resulting in the $Ni/Al_3Ni_2/Al_3Ni/Al_3Ni_2/Ni$ joint formation, Figure 8b

The solidification path $N_0 \rightarrow N^F$, is situated on the *liquidus* line of the meta-stable equilibrium phase diagram calculated for the solidification, Figure 9.

The N^F – parameter shown in Figure 1, Figure 3 and Figure 6a was measured by means of the EDAX technique, Figure 10a, ($N^F_{\exp.}$) and next, it was determined theoretically, Figure 10b, ($N^F_{theor.}$). Additionally, solute concentration in the zones *ss* and *s* is determined for a given T_R – isotherm.

The $N^F_{theor.}$ – value was determined as the intersection of the T_T – isotherm and *liquidus* line of the phase diagram for meta-stable equilibrium, Figure 10b.

The *ss* – point results from the intersection of the T_R – isotherm and *solidus* line which is drawn in the meta-stable equilibrium phase diagram calculated for dissolution, while *s* – point is determined by *solidus* line of the meta-stable equilibrium phase diagram for solidification.

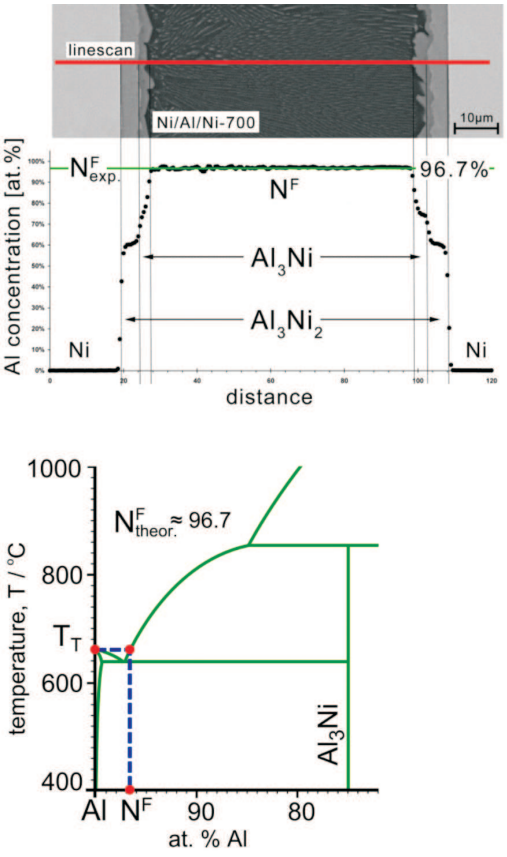

Fig. 10. Method of determination of the N^F – parameter: a/ experimentally with Ni/Al/Ni-700 interconnection for which solidification was arrested and morphology frozen, b/ due to the Al-Ni meta-stable equilibrium phase diagram, (T_T is the Al – melting point, N^F – is the solution of the Ni in the Al – filler metal, as shown in Figure 1)

5. Drift of the system towards the thermodynamic equilibrium

The analyzed Ni/Al_3Ni_2/Al_3Ni/Al_3Ni_2/Ni joint was obtained under meta-stable condition. This is a natural tendency of this kind of systems to achieve a thermodynamic equilibrium. The equilibrium would be reached when the analyzed Ni/Al_3Ni_2/Al_3Ni/Al_3Ni_2/Ni joint is transformed into Ni/(Ni)/Ni joint. Therefore, some solid / solid transformations are needed. The first transformation in sequence was observed in the studied joint, Figure 11.

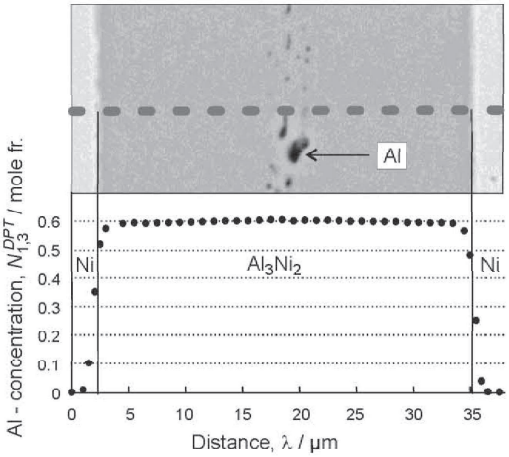

Fig. 11. EDS observation of the full consumption of the Al_3Ni coupled phase by the Al_3Ni_2 dominant phase according to reaction: $2Al_3Ni \rightarrow Al_3Ni_2 + 3Al$; the pure Al precipitates diffuse towards the joint axis of symmetry

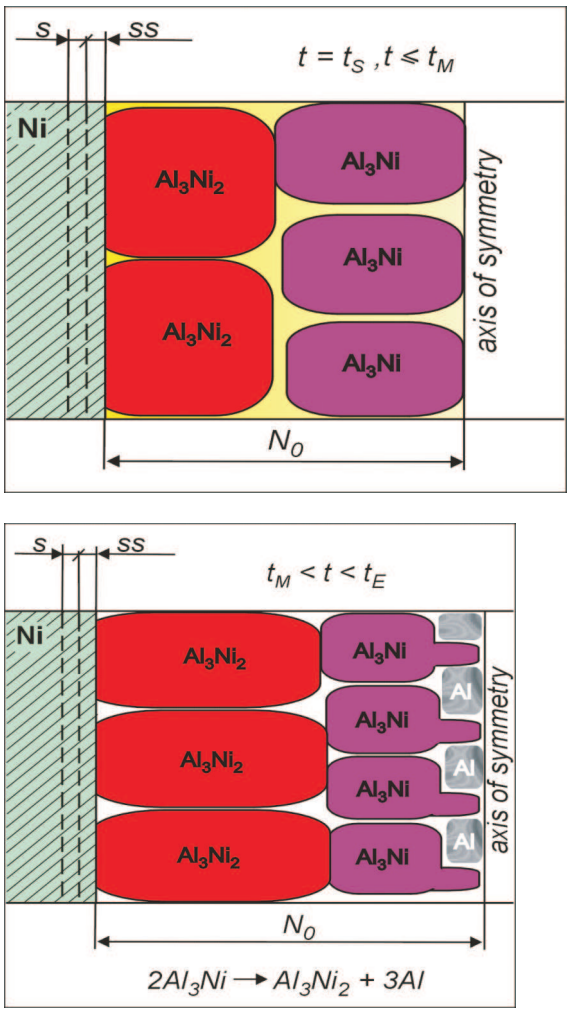

Fig. 12. Half the diffusion joint Ni/Al_3Ni_2/Al_3Ni/Al_3Ni_2/Ni; a/ just at the completion of solidification, $t_S \equiv t^F$; zone dx disappeared; b/ during the first solid / solid transformation; N_0 – parameter is the same for both analyzed phenomena

The mass balance measured at different solidification times confirms that the N_0 – solute concentration is conserved during all solidification time, Figure 6. The characteristic N_0 – solute concentration is shown schematically for the completed solidification, Figure 12a.

However, it should be emphasized that the mentioned N_0 – solute concentration is also conserved during the so-called "*mantis phenomenon*", Figure 12b. It is evident that the system became closed and no exchange of the mass between substrate and joint is possible during this first solid / solid transformation.

The cells of both Al_3Ni_2 and Al_3Ni phases are always visible inside the proper sub-layers. The cellular morphology of cells shown schematically in Figure 12 were confirmed experimentally due to the SEM analysis applied to the joint frozen during arrested solidification [10].

6. Concluding remarks

1/ regardless of the real temperature, T_R, imposed in the technology, (Table 1), the beginning of solidification path is always the same, and is equal to N_0,

2/ regardless of the real temperature, T_R, the end of solidification path is always the same and is equal to N^F, which was confirmed experimentally, Figure 10a, and predicted theoretically, Figure 10b; a good agreement was obtained between both $N^F_{(exp.)}$ and $N^F_{(theor.)}$ parameters,

3/ the N_0 – solute concentration is created within the zone dx as a result of dissolution, Figure 1-2,

4/ the N_0 – solute concentration is reproduced subsequently within the joint as an average solute concentration, Table 1,

5/ the N_0 – solute concentration created within the zone dx corresponds well to the N_{min} – solute concentration which is manifested by the meta-stable equilibrium phase diagram for dissolution, Figure 8, $N_0 \approx N_{min}$,

6/ the N_0 – solute concentration plays essential role in the competition between stable and meta-stable formation of the interconnection, Figure 7,

7/ the N_0 – solute concentration located on the *liquidus* line, Figure 3, is treated as an initial condition for the differential equation which describes the solidification,

8/ according to the current model assumption, creation of the zone dx, follows the reaction: $N^F + Ni \rightarrow s(N^s) + ss(N^s s) + dx(N_0)$, as drawn in Figure 13,

9/ according to the meta-stable equilibrium phase diagram, Figure 9, the first Al_3Ni_2 – intermetallic phase sub-layer (in sequence of appearance) is formed due to the phenomenon of partitioning along the solidification path $N_0 \Rightarrow N_2^M$, (it is marked in Figure 13), and diffusion into the solid; a simulation of the Al_3Ni_2 – intermetallic phase sub-layer is shown in Figure 14,

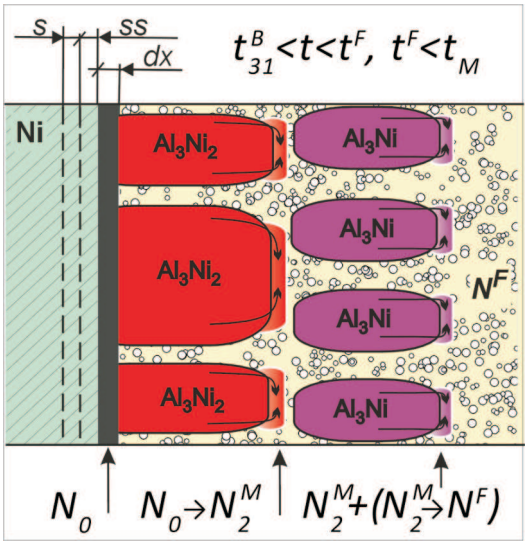

Fig. 13. Localization of the zone dx, zone ss and zone s within the Ni – substrate

10/ according to the same phase diagram, Figure 9, the second Al_3Ni – intermetallic compound sub-layer is formed due to the reaction between the N_2^M – liquid and Al_3Ni_2 primary phase, ($x_1^{max} - x_1^{min}$ in Figure 14) next due to the partitioning along the solidification path $N_2^M \rightarrow N^F$, ($x_2 - x_1^{max}$ in Figure 14) with diffusion into the solid, (it is marked in Figure 13),

11/ localizations of the N_2^M – liquid and Al_3Ni_2 primary phase in the growing joint suggest that peritectic reaction (not peritectic transformation) takes place to form Al_3Ni – compound at the N_2^M – point, Figure 9, (according to the description by Phelan *et al.* [11]),

12/ the Gibbs Phase Rule applied to the current model and experimental observations yields the Number of Degrees of Freedom $l = 0$, as required for the isothermal solidification imposed to the joint technology: $l = c - p + 1$; thus $l = c - p + 1 = 0$, with $c \equiv Ni, Al$, therefore, $p = 3$,

13/ in fact, $p \equiv liquid(N_0)_d x, Al_3Ni_2, Al_3Ni = 3$, as it is justified by the current model and adequate experiments, Figure 6, Figure 10a,

14/ the model is universal one and can be applied to other situations where the brazing is expected; it is suggested that brazing occurs in the case of massive rolls solidification, when the solid core interacts on the surrounding liquid steel added in the second step of the technology.

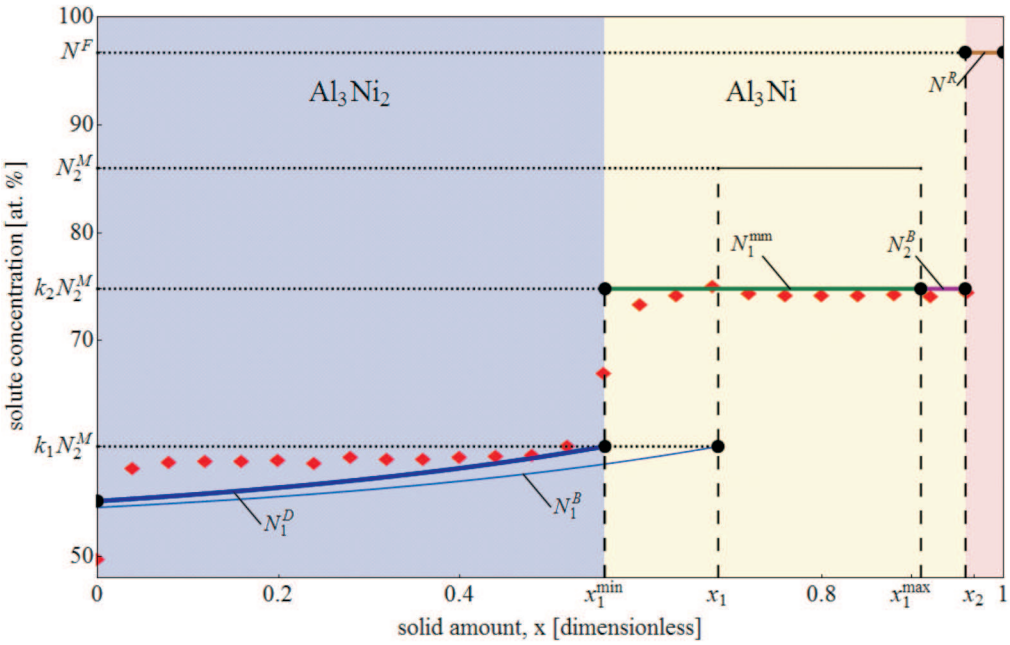

Fig. 14. Simulation of both sub-layers formation; x_1 – amount of the Al_3Ni_2 primary phase formed due to solidification path $N_0 \Rightarrow N_2^M$ shown in Figure 9; $x_1^{max} - x_1^{min}$ – amount of the Al_3Ni – compound formed due to the undercooled peritectic reaction at N_2^M – point on solidification path: $(x_1 - x_1^{min})[k_1N_2^M] + (x_1^{max} - x_1)[N_2^M] \Rightarrow (x_1^{max} - x_1^{min})[k_2N_2^M]$; $x_2 - x_1^{max}$ – amount of Al_3Ni – compound formed due to the partitioning along the solidification path $N_2^M \rightarrow N^F$ shown in Figure 9, Eq. (5C); N^F – remaining last part of the liquid which returns back to the process of dissolution; N^D – theoretical solute redistribution within the Al_3Ni_2 primary phase, Eq. (6P); $k_2N_2^M$ – solute redistribution within the Al_3Ni – compound; measurement point are marked by red squares

Acknowledgements

The financial support from the Polish Ministry of Science and Higher Education (MNiSW – Poland) under the contract: N R15 006 004 is gratefully acknowledged.

Appendix

The following mathematical formalism was applied to the current model:

1/ formation of the intermetallic phase, $k_i^L = 0$

The solute concentration in the liquid, changes during precipitation of primary phases along a given local solidification path, i, in accordance with the relationship:

$$\mathrm{N_i^L}\left(\mathrm{x};\alpha_\mathrm{i}^\mathrm{D},\mathrm{l_i^0},\mathrm{N_{i-1}},\mathrm{k_i^0}\right) = \mathrm{N_{i-1}}\left[\frac{\mathrm{l_i^0}+\alpha_\mathrm{i}^\mathrm{D}\mathrm{k_i^0}\mathrm{x}-\mathrm{x}}{l_i^0}\right]^{\frac{\mathrm{k_i^0}-1}{1-\alpha_i^D k_i^0}} \tag{1P}$$

The Eq. (1P) is the solution to differential equation for solidification/micro-segregation:

$$dN_i^L/dx = (1-k_i^0)N_i^L(x)/(l_i^0 + \alpha_i^D k_i^0 x - x) \tag{2P}$$

with the initial condition:

$$N_i^L(0;\alpha_i^D, l_i^0, N_(i-1), k_i^0) = N_(i-1) \tag{3P}$$

The phenomenon of partitioning results in the formation of the solid / liquid interfaces, and "history" of the solute concentration at the existed interfaces are given as:

$$N_i^S(x;\alpha_i^D, l_i^0, N_(i-1), k_i^0) = k_i^0 N_i^L(x;\alpha_i^D, l_i^0, N_(i-1), k_i^0) \tag{4P}$$

The phenomenon of back-diffusion superposes solute partitioning. The superposition of both phenomena results in the solute redistribution, which is the function of the solute concentration at formerly (historically) existing solid / liquid interfaces.

$$N_i^B(x;x_i^0,\alpha_i^D, l_i^0, N_(i-1), k_i^0) = [1+\beta_i^{ex}(x;x_i^0, l_i^0, k_i^0)\beta_i^{in}(x_i^0;\alpha_i^D, l_i^0, k_i)] N_i^S(x;\alpha_i^D, l_i^0, N_(i-1), k_i^0)$$

The peritectic reaction requires the so-called "shifted redistribution" formed within the primary phase:

$$N_i^D(x;x_i^0,\alpha_i^D, l_i^0, N_(i-1), k_i^0) = [N_i^B(x+x_i-x_i^{min};\alpha_i^D, l_i^0, N_(i-1), k_i^0)] \tag{6P}$$

2/ general description of the intermetallic phase / compound formation, with $k_i^0 \neq 0$; $k_i^L \neq 0$

The solute concentration in the liquid, changes during precipitation of primary phases along the given local solidification path, i, in accordance with the relationship:

$$\begin{aligned}&\mathrm{N_i^L(x;\alpha_i^D, l_i^0, N_{i-1}, k_i)} = [\mathrm{N_{i-1}/(1-k_i^0)}]\\ &\left\{\mathrm{k_i^L + (1-k_i^0 - k_i^L)[(l_i^0 + \alpha_i^D k_i^0 x - x)/l_i^0]^{\frac{k_i^0-1}{1-\alpha_i^D k_i^0}}}\right\}\end{aligned} \quad (1G)$$

Eq. (1C) is the solution to differential equation for solidification/micro-segregation:

$$dN_i^L/dx = [(1-k_i^0)N_i^L(x) - k_i^L N_(i-1)]/(l_i^0 + \alpha_i^D k_i^0 x - x) \quad (2G)$$

with the initial condition:

$$N_i^L(0;\alpha_i^D, l_i^0, N_{i-1}, k_i^0, k_i^L) = N_{i-1} \quad (3G)$$

The "history" of solute concentration, at the appearing interfaces is described as follows:

$$N_i^S(x;\alpha_i^D, l_i^0, N_{i-1}, k_i) = k_i^0 N_i^L(x;\alpha_i^D, l_i^0, N_{i-1}, k_i) + k_i^L N_{i-1} \quad (4G)$$

Consequently, the solute redistribution after partitioning and back-diffusion is given by:

$$\begin{aligned}&\mathrm{N_i^B(x; x_i^0, \alpha_i^D, l_i^0, N_{i-1}, k_i)} =\\ &\left[1+\beta_i^{\mathrm{ex}}(\mathrm{x; x_i^0, l_i^0, k_i})\beta_i^{\mathrm{in}}(\mathrm{x_i^0, \alpha_i^D, l_i^0, k_i})\right]\mathrm{N_i^S(x;\alpha_i^D, l_i^0, N_{i-1}, k_i)}\end{aligned} \quad (5G)$$

3/ formation of the intermetallic compound, $k_i^0 = 0$

The general formulation of the differential equation is:

$$\begin{aligned}dN_i^L/dx =&[(1-k_i^0)N_i^L - k_i^L N_{i-1}]\\ &/(l_i^0 + \alpha_i^D(k_i^0 + k_i^L[N_{i-1}/N_i^L(x)]x - x)\end{aligned} \quad (0C)$$

Its simplified form appropriate to the formation of the intermetallic phase (with $k_i^L = 0$) is presented by Eq. (1P). However, its simplified form adequate to the formation of the intermetallic compound can be obtained by introduction of the $k_i^0 = 0$ into the Eq. (0C). Then, the following differential formula is to be obtained:

$$dN_i^L/dx = [N_i^L - k_i^L N_{i-1}]/(l_i^0 + \alpha_i^D(k_i^L[N_{i-1}/N_i^L(x)]x - x) \quad (1C)$$

which is to be solved with the initial condition:

$$N_i^L(0;\alpha_i^D, l_i^0, N_{i-1}, k_i^L) = N_{i-1} \quad (2C)$$

to obtain the function $N_i^L(x)$ which can be calculated numerically for a given value of the x:

$$x = l_i^0\{AB + C\}[M]^{-1} \quad (3C)$$

where

$$\begin{aligned}A =& N_0^{\alpha_i^D+1}\left[N_i^L(x)\right]^{-\alpha_i^D}\left(N_0 - N_2^M k_i^L\right)^{-\alpha_i^D}\\ &\left[\alpha_i^D {}_2F_1\left(l, l; \alpha_i^D + 2; N_0\left(N_2^M k_i^L\right)^{-1}\right) - \alpha_i^D - 1\right]\end{aligned} \quad (a3C)$$

$$B = \left(N_i^L(x) - N_2^M k_i^L\right)^{\alpha_i^D} \quad (bC)$$

$$\begin{aligned}C =& N_i^L(x)\\ &\left[\alpha_i^D\left(-{}_2F_1\left(l.l; \alpha_i^D + 2; N_i^L(x)\left(N_2^M k_i^L\right)^{-1}\right)\right) + \alpha_i^D + l\right]\end{aligned} \quad (c3C)$$

$$M = \left(N_i^L(x) - N_2^M k_i^L\right)\left(\alpha_i^D + l\right) \quad (d3C)$$

The "history" of solute concentration, at the appearing interfaces is described as follows:

$$N_i^S\left(x;\alpha_i^D, l_i^0, N_{i-1}, k_i^L\right) = k_i^L N_i^L\left(x;\alpha_i^D, l_i^0, N_{i-1}, k_i^L\right) \quad (4C)$$

The solute redistribution of the formed intermetallic compound is equal to solute concentration at the appearing solid / liquid interfaces:

$$N_i^B\left(x; x_i^0, \alpha_i^D, l_i^0, N_{i-1}, k_i^L\right) \equiv N_i^S\left(x;\alpha_i^D, l_i^0, N_{i-1}, k_i^L\right) \quad (5C)$$

There is no need to calculate the amount of peritectic reaction because the intermetallic compound is formed due to the partitioning phenomenon, only.

All the above relationships Eq. (1P-6P), Eq. (1G-5G) and Eq. (1C-5C) are formulated with the use of:

$$l_i^0 = \begin{cases} L^0, i = 1;\\ L^0 - \sum_{j=1}^{i=1} x_j^{max}, i = 2, \ldots, n;\end{cases} \quad (1A)$$

$$x_i^0 = \begin{cases} X^0, i = 1;\\ X^0 - \sum_{j=1}^{i=1} x_j^{max}, i = 2, \ldots, n;\end{cases} \quad (2A)$$

Additionally, the following definition of the coefficient of the redistribution extent was formulated;

$\beta_i^{ex}(x; x_i^0, l_i^0, k_i)$ is the solution to the following equation:

$$(1+\beta_i^{ex})N_i^S(x; 1, l_i^0, N_{i-1}, k_i) = N_i^S(x_i^0; 1, l_i^0, N_{i-1}, k_i) \quad (3A)$$

Moreover, the definition of the coefficient of the redistribution intensity was also formulated;

$\beta_i^{in}(x_i^0; \alpha_i^D, l_i^0, k_i)$ is the solution to the following equation:

$$\begin{aligned}&\int_0^{\mathrm{x_i^0}}\left[1+\beta_{\mathrm{i}}^{\mathrm{in}}\beta_{\mathrm{i}}^{\mathrm{ex}}(\mathrm{x; x_i^0, l_i^0, k_i})\right]\mathrm{N_i^S(x;\alpha_i^D, l_i^0, k_i)dx}\\ &= \mathrm{l_i^0 N_{i-1} - (l_i^0 - x_i^0)N_i^L(x_i^0;\alpha_i^D, l_i^0, N_{i-1}, k_i)}\end{aligned} \quad (4A)$$

REFERENCES

[1] I. Tuah-Poku, M. Dollar, T. Massalski, A Study of the Transient Liquid Phase Bonding Process Applied to a Ag/Cu/Ag Sandwich Joint, Metallurgical Transactions **19A**, 675-686 (1988).

[2] J. Kloch, E. Guzik, J. Janczak-Rusch, D. Kopyciński, T. Rütti, J. Kim, H.M. Lee, W. Wołczyński, Morphological Characteristics of the Multi-layer/Substrate Systems, Proceedings of the 9th European Congress on Stereology and Image Analysis, Zakopane (Poland), 375-382 (2005).

[3] W. Wołczyński, E. Guzik, D. Kopyciński, T. Himemiya, J. Janczak-Rusch, Mass Transport during Diffusion Soldering or Brazing at the Constant Temperature, Proceedings of the 13th International Heat Transfer Conference – Sydney (Australia), (2006), ed. begell house, eds. G.de Vahl Davis & E.Leonardi,CD, MST-11, 12 pages.

[4] Y.K. Chuang, D. Reinisch, K. Schwerdtfeger, Kinetics of Diffusion Controlled Peritectic Reaction during Solidification of Iron-Carbon Alloys, Metallurgical Transactions **6(A)**, 235-238 (1975).

[5] D.M. Jacobson, G. Humpston, Diffusion Soldering, Soldering & Surface Mount Technology **10**, 27-32 (1992).

[6] R. Jiangwei, L. Yajiang, F. Tao, Microstructure Characteristics in the Interface Zone of Ti/Al Diffusion Bonding, Materials Letters **56**, 647-652 (2002).

[7] W. Wołczyński, J. Kloch, J. Janczak-Rusch, K. Kurzydłowski, T. Okane, Segregation Profiles in Diffusion Soldered Ni/Al/Ni Interconnections, Materials Science Forum **508**, 385-392 (2006).

[8] D. Kopyciński, Krystalizacja faz międzymetalicznych i cynku na żelazie oraz jego nisko- i wysokowęglowych stopach podczas procesu cynkowania. Monografia AGH, 149, Kraków 2006, 131 stron.

[9] T. Umeda, T. Okane, W. Kurz, Phase Selection during Solidification of Peritectic Alloys, Acta Materialia **44**, 4209-4216 (1996).

[10] W.D. MacDonald, T.W. Eagar, Isothermal Solidification Kinetics of Diffusion Brazing, Metallurgical and Materials Transactions **29A**, 315-325 (1998).

[11] D. Phelan, M. Reid, R. Dippenaar, Kinetics of the Peritectic Phase Transformation: In-situ Measurements and Phase Field Modelling, Metallurgical/Materials Transactions **37A**, 985-989 (2006).

Received: 10 December 2010.